machines

MDPI

Article

PDA Nanoparticle-Induced Lubricating Film Formation in Marine Environments: An Active Approach

Xinqi Zou, Zhenghao Ge, Chaobao Wang * and Yuyang Xi

College of Mechanical and Electrical Engineering, Shaanxi University of Science and Technology, Xi'an 710021, China; bs210511001@sust.edu.cn (X.Z.); gezh@sust.edu.cn (Z.G.); xyy2497389994@163.com (Y.X.)
* Correspondence: chaobaowang@sust.edu.cn

Abstract: The low viscosity of water-lubricated films compromises their load-bearing capacity, posing challenges for practical application. Enhancing the lubrication stability of these films under load is critical for the successful use of seawater-lubricated bearings in engineering. Polydopamine (PDA) shows great potential to address this issue due to its strong bio-inspired adhesion and hydration lubrication properties. Thus, PDA nanoparticles and seawater suspensions were synthesized to promote adhesive lubricating film formation under dynamic friction. The lubrication properties of PDA suspensions were evaluated on Cu ball and ultra-high molecular weight polyethylene (UHMWPE) tribo-pairs, with a detailed comparison to seawater. The results show PDA nanoparticles provide excellent adhesion and lubrication, enhancing the formation of lubricating films during friction with seawater. Under identical conditions, PDA suspensions demonstrated the lowest friction coefficient and minimal wear. At 3 N, friction decreased by 56% and wear by 47% compared to distilled water. These findings suggest a novel strategy for using PDA as a lubricant in seawater for engineering applications.

Keywords: polydopamine; seawater; underwater adhesion; lubrication

check for updates

Citation: Zou, X.; Ge, Z.; Wang, C.; Xi, Y. PDA Nanoparticle-Induced Lubricating Film Formation in Marine Environments: An Active Approach. *Machines* **2024**, *12*, 817. https://doi.org/10.3390/machines12110817

Received: 19 September 2024
Revised: 11 October 2024
Accepted: 16 October 2024
Published: 16 November 2024

1. Introduction

Water-lubricated bearings, critical propulsion components for environmentally sustainable ocean vessels, provide significant advantages, including environmental protection and cost-effectiveness [1,2]. However, their adoption in practical applications remains significantly limited compared to oil-lubricated bearings, primarily due to the inherent low load capacity and lubrication stability resulting from water's low viscosity [3]. This limitation leads to significant friction and wear during the operation of water-lubricated bearings, particularly during critical startup and shutdown phases [4,5]. Consequently, enhancing the stability of the lubricating film within a low-viscosity water environment is essential for the technological advancement and broader implementation of water-lubricated bearings.

Hydration lubrication represents a highly efficient form of water-based lubrication, capable of achieving ultralow friction and minimal wear [6,7]. Hydration lubrication relies on the formation of a hydration layer by water molecules on solid surfaces. This layer provides a thin film of water between friction contact surfaces, thereby reducing direct solid-to-solid contact. The hydration layer facilitates a flowing environment, allowing for smoother sliding between the contact surfaces while significantly lowering the friction coefficient. In pursuit of identifying effective strategies for applying hydration lubrication in water-lubricated engineering applications, researchers previously synthesized and tested a series of soft matter microparticle and UHMWPE composites [8–11]. The findings indicate that the hydration lubrication provided by soft matter substantially reduces the friction coefficient and wear mass loss in friction pairs when utilizing a water tank as the lubricating medium. However, in practical applications, most water-lubricated bearings operate within an open lubrication system. Therefore, maintaining the stability of the hydration

lubrication film between interacting surfaces will be a pivotal area of focus for future research endeavors.

As an outstanding mussel-inspired material, polydopamine (PDA) exhibits the remarkable ability to adhere to nearly any surface within a seawater environment [12–15]. Furthermore, PDA significantly mitigates friction and wear behaviors across various materials when applied as a surface coating under water lubrication conditions [16]. Our relevant research also shows that PDA effectively integrates the functions of bionic adhesion and hydration lubrication within distilled water environments. Considering that ocean-going vessels encounter harsher operating conditions, demand higher reliability, and rely heavily on water-lubricated bearings, it becomes imperative to investigate the lubricating properties of PDA under seawater conditions.

In conclusion, the use of PDA offers an effective solution to the aforementioned challenges and demonstrates the potential of PDA as a green lubricant for seawater-lubricated bearings [16–22]. Additionally, UHMWPE and copper alloy are particularly well-suited for the manufacture of various water-lubricated bearings. In this study, PDA nanoparticles with unique small size effects and efficient transfer capabilities were synthesized in seawater and alkaline aqueous solutions, respectively. The tribological performance of the friction pairs and the lubricating properties of PDA nanoparticles were experimentally tested and analyzed in seawater environments. The obtained results present a novel approach to achieving targeted lubrication films derived from PDA nanoparticles under seawater conditions, benefiting the operational performance of undersea engineering devices, such as water-lubricated bearings.

2. Methodology

2.1. Raw Materials

Ethanol (analytical reagent), artificial seawater, and distilled water were sourced from Shanghai Aladdin Biochemical Technology Co., Ltd. (Shanghai, China). The triethanolamine was procured from Sinopharm Chemical Reagent Co., Ltd. (Shanghai, China). The dopamine hydrochloride (Alfa-A11136) was supplied by Thermo Fisher Scientific Co., Ltd. (Waltham, MA, USA). The dialysis membrane was obtained from Sinopharm Chemical Reagent Co., Ltd.

2.2. Preparation of PDA Nanoparticles and Composites

Dopamine hydrochloride (200 mg) was dissolved in a mixed solvent consisting of deionized water (250 mL) and ethanol (50 mL), and the pH was adjusted to 8.5 using triethanolamine. PDA nanoparticles were synthesized through the self-polymerization of dopamine monomers within a dialysis membrane, under stirring conditions of 100 r/min for 24 h at room temperature. To remove the triethanolamine from the mixed solvent, the PDA nanoparticle suspensions were poured and sealed into dialysis membranes, followed by immersion in distilled water with continuous stirring for 24 h. The prepared PDA nanoparticle suspensions were purified for three times, and dry PDA nanoparticles were obtained by vacuum freeze-drying method. Distilled water and seawater suspensions were prepared by dispersing dry PDA nanoparticles into distilled water and seawater, respectively. Five seawater suspensions with varying PDA concentrations (0.1 mg/mL, 0.25 mg/mL, 0.5 mg/mL, 0.75 mg/mL, and 1 mg/mL) were prepared and named PDA-1, PDA-2, PDA-3, PDA-4, and PDA-5, respectively. The preparation process of PDA nanoparticles is shown in Figure 1.

2.3. Characterization of PDA Nanoparticles and Worn Surfaces

The particle sizes and surface topographies of PDA nanoparticles were examined using the scanning electron microscope (VEGA3, Tescan China, Ltd., Shanghai, China). The chemical structures of PDA nanoparticles were analyzed through infrared absorption spectroscopy (Nicolet 6700, Thermo Electron Scientific Instruments, Ltd., Waltham, MA, USA).

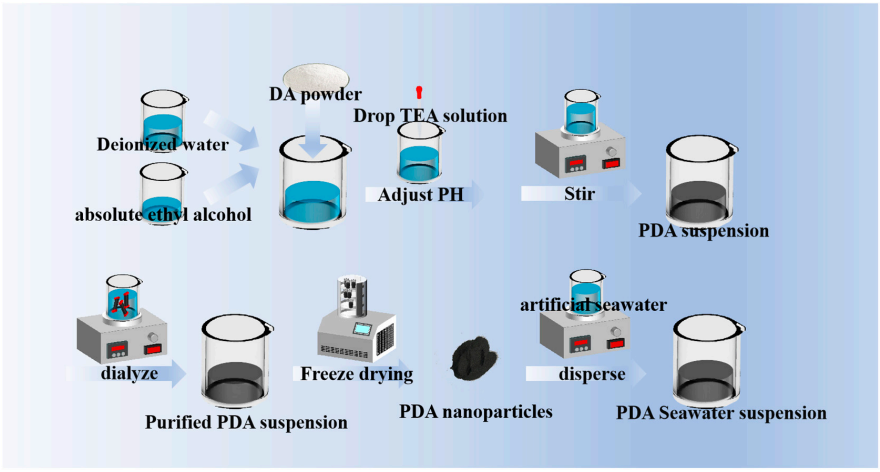

Figure 1. Preparation process of PDA nanoparticles.

2.4. Friction and Wear Testing

In consideration of the actual manufacturing conditions of ship tail shaft bushings and water-lubricated bearings, QSn4–3 copper and UHMWPE were selected as the materials for the two friction pairs used in the rubbing tests. As illustrated in Figure 2a, the QSn4–3 copper balls were machined to a diameter of 6 ± 0.05 mm, while the UHMWPE disks were machined to a diameter of 20 ± 0.05 mm and a thickness of 6 ± 0.05 mm. Friction and wear tests were performed using a ball-on-disk wear tester (MFT-5000, Rtec Instruments Co., Ltd., San Jose, CA, USA) to evaluate the lubricating properties of PDA nanoparticles in seawater, with the wear rates of the UHMWPE disks calculated using Equation (1). To better simulate the actual working conditions, loads of 0.5, 1, and 3 N, along with a relatively low sliding velocity of 100 mm/s, were applied to assess the lubrication performance of both water and PDA solutions. All the friction and wear tests were repeated three more times to ensure the accuracy of testing data. The schematic diagram of the rubbing tests is presented in Figure 2.

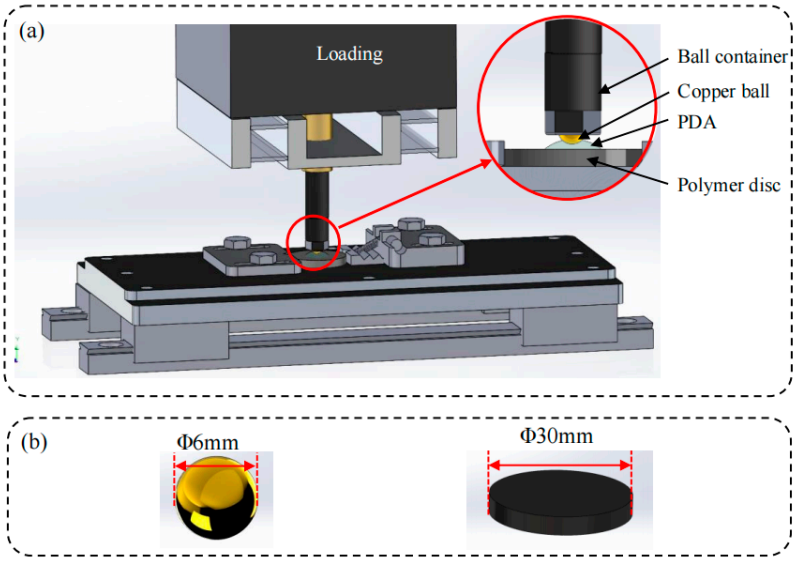

Figure 2. Schematic illustration of the test apparatus. (**a**) Schematic diagram of the friction tester (**b**) Schematic diagram of the copper ball and disk.

2.5. Worn Surfaces

The characteristics and roughness of worn surfaces were thoroughly examined using SEM and 3D laser confocal microscope (VK-X2000, Keyence Ltd., Osaka, Japan). The

presence of PDA films adhered to the worn surfaces was confirmed using an energy dispersive spectrometer (EDS) integrated into the SEM instrument. The wear rates were calculated from Equation (1).

$$\text{Wear rate} = \frac{\text{Volume loss}}{\text{Load} \times \text{Sliding distance}} \left(\text{mm}^3\text{N}^{-1}\text{m}^{-1}\right) \quad (1)$$

3. Results

3.1. Analysis and Characterization of PDA Microspheres

To elucidate the adhesion and lubrication mechanisms of PDA nanoparticles, we employed scanning electron microscopy (SEM) and Fourier transform infrared (FTIR) spectroscopy to analyze their morphology, size, and chemical structure, as shown in Figure 3. Figure 3 demonstrates the morphology and size of PDA nanoparticles, which appear spherical, partially aggregated, and irregularly dispersed. The diameters of 100 PDA nanoparticles were randomly measured in the SEM images, yielding an average diameter of 280.36 ± 50 nm. The formation of nanoparticles indicates that dopamine undergoes self-polymerization.

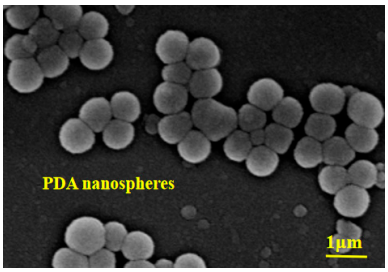

Figure 3. SEM images of microsized PDA particles.

The positions of the absorption peaks in the IR spectra of PDA nanoparticles are presented in Figure 4. The chemical structure of the PDA nanoparticles can be elucidated from the absorption peak values. The spectrum exhibits a peak at 1590 cm^{-1}, corresponding to the bending vibration of the N-H bond on the aromatic ring. The peak at 1470 cm^{-1} corresponds to the bending vibration of the carbon atoms on the benzene ring. The peak at 1292 cm^{-1} corresponds to the stretching vibration of the carbon atoms on the benzene ring. The shear vibration of the N-H bond is observed at 1510 cm^{-1}. The expansion and contraction vibrations of O-H and N-H are represented by the large peak of 3200 cm^{-1}. The occurrence of peaks in the characteristic functional groups of dopamine also suggests the occurrence of self-polymerization. The self-polymerization process of dopamine hydrochloride is shown in Figure 5. Dopamine undergoes oxidation of its phenolic hydroxyl group (-OH) in the presence of air or oxidizing agents, leading to the formation of quinone. Quinone can react with other dopamine molecules or its own quinone form, resulting in the formation of longer polymer chains.

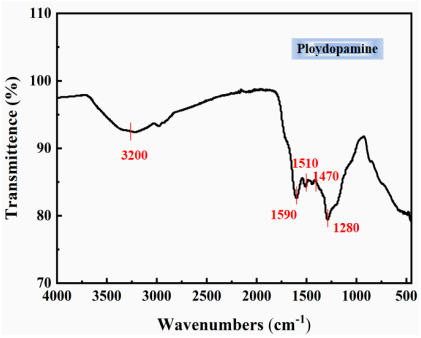

Figure 4. Infrared spectrum of PDA.

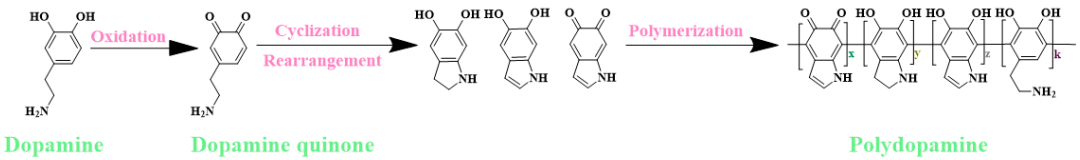

Figure 5. Self-polymerization process of dopamine hydrochloride.

3.2. Effect of Stirring Rate on Particle Size of PDA Microspheres

To further explore the self-polymerization and lubrication mechanism of PDA with a view to controlling the diameter of PDA nanoparticles polymerized under seawater environment by stirring rate, we prepared PDA nanoparticles at stirring rates of 100 r/min, 200 r/min, 300 r/min, 400 r/min, 500 r/min, and 600 r/min. Their particle size distributions are shown in Figure 6. As the stirring rate increased, the diameter of PDA nanoparticles, particularly those accounting for a significant proportion, exhibited an upward trend, and the distribution range of particle sizes also expanded accordingly.

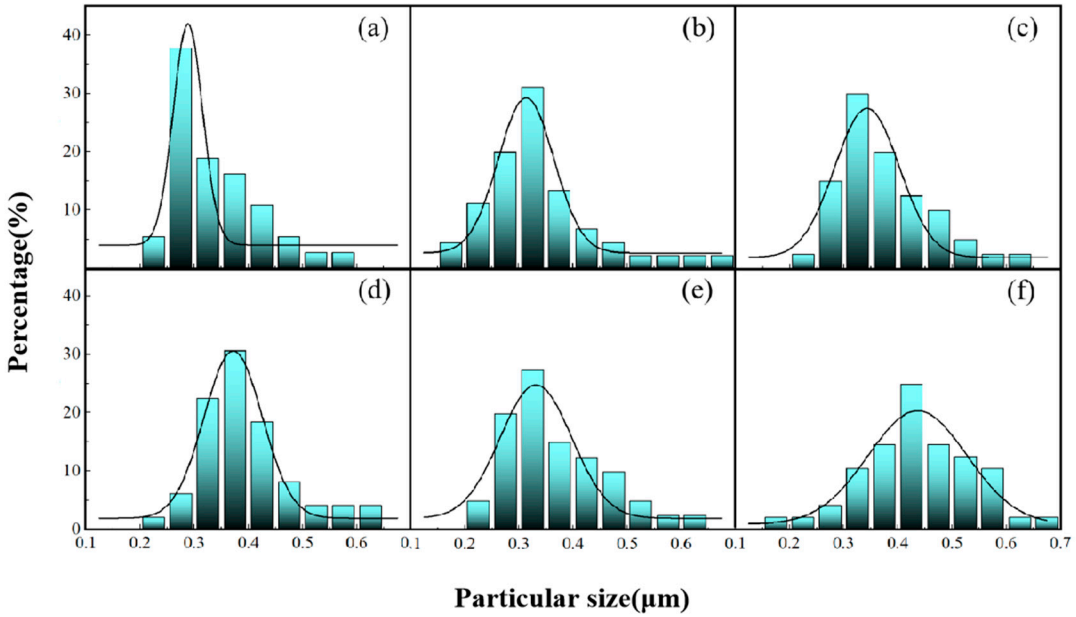

Figure 6. The effects of speed on the particle size: (**a**) 100 r/min, (**b**) 200 r/min, (**c**) 300 r/min, (**d**) 400 r/min, (**e**) 500 r/min, (**f**) 600 r/min.

3.3. Analysis of Friction Coefficients

To better understand the lubricating mechanism of PDA nanoparticles in a seawater environment, the friction coefficients of UHMWPE and copper friction pairs under different PDA seawater suspensions lubrication were tested and analyzed. The effects of testing conditions on the friction properties of the friction pairs were also evaluated. As illustrated in Figure 7a–c, all friction coefficients show a similar increasing trend at the primary stage of the rubbing process and then approached to a flat. This occurs because the running-in process of the rough friction pair surfaces leads to an increase in friction coefficients. It can also be observed that the friction pairs exhibit the highest friction coefficients when seawater is used as the lubricant under identical testing conditions. This illustrates that PDA nanoparticles added to seawater have satisfactory lubricating performance, effectively reducing friction and wear during rubbing processes. It is also noteworthy that the lubricating performance of PDA seawater suspensions improves with increasing PDA concentration when the concentration is below 0.25 mg/mL. However, the lubricating ability of PDA seawater suspension drops with the continuous increase of PDA concentration when PDA concentration is more than 0.25 mg/mL. This indicates that both too high and

too low a PDA concentration have an adverse effect on its lubricating ability. The optimum PDA concentration is 0.25 mg/mL under the testing conditions.

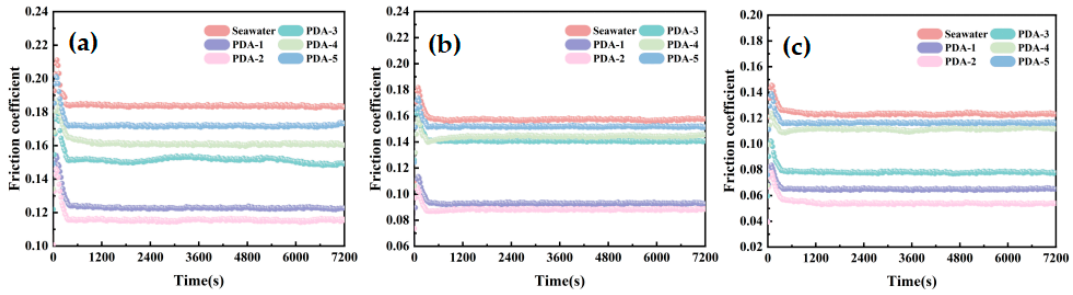

Figure 7. Friction coefficients of polymer disks under various loads: (**a**) 0.5 N, (**b**) 1 N, (**c**) 3 N.

Figure 8a illustrates the trend of average friction coefficients under three different normal loads. As depicted in Figure 8a, the average friction coefficient exhibits a decreasing trend with increasing normal load. This observation is consistent with our previous research on the tribological behavior of UHMWPE and copper friction pairs. Additionally, it can be observed that the friction pairs have a lower friction coefficient when using PDA seawater suspension as lubricant. This demonstrates that PDA nanoparticles dispersed in seawater provide excellent lubricating performance.

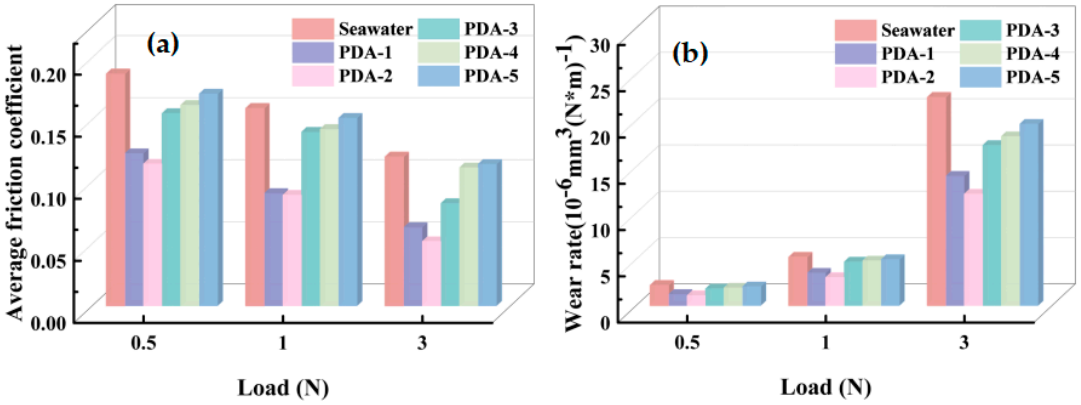

Figure 8. Average friction coefficient (**a**), wear rates (**b**) of UHMWPE polymer disks at various applied loads.

To accurately analyze the friction and wear behaviors, the wear rates were calculated based on the testing results. As shown in Figure 8b, the UHMWPE disk lubricated with PDA suspension exhibits a lower wear rate than the UHMWPE disk lubricated with seawater under the same testing conditions. This demonstrates that PDA nanoparticles added to seawater can effectively reduce the wear behaviors of friction pairs during the rubbing process. It also can be seen that the PDA suspensions with concentrations of 0.1 and 0.25 mg/mL have better lubricating capacity under the three loads. In addition, the wear rate of UHMWPE disks under low load of 0.5 N has a larger drop than that of UHMWPE disks under relatively high loads of 1 and 3 N. This demonstrates that the lubricating capacity of PDA nanoparticles has more efficiency under the low load of 0.5 N. It could be attributed to the adhesive force of PDA nanoparticles being insufficient to withstand the shear stress during the rubbing process when the normal load exceeds 1 N. Consequently, this destabilizes the PDA lubrication and results in relatively high wear rates.

3.4. Analysis of Worn Surfaces

To further analyze the lubrication behavior of PDA nanoparticles, three-dimensional surface topography was employed to examine the wear patterns of the UHMWPE disks

after friction testing under a 3 N load, as illustrated in Figure 8. The experimental results indicated that the surface abrasion depths of the UHMWPE disks in the PDA-enhanced seawater suspension were consistently smaller than those in the seawater-only environment. Notably, the UHMWPE disk exhibited the shallowest abrasion depth and width at a PDA concentration of 0.25 mg/mL. As the PDA content increased, the width and depth of the abrasion marks on the UHMWPE disks exhibited an upward trend. At a PDA concentration of 1 mg/mL, significant micro-pit defects were observed on the wear surface of the UHMWPE disk, consistent with the results and trends presented in Figure 9.

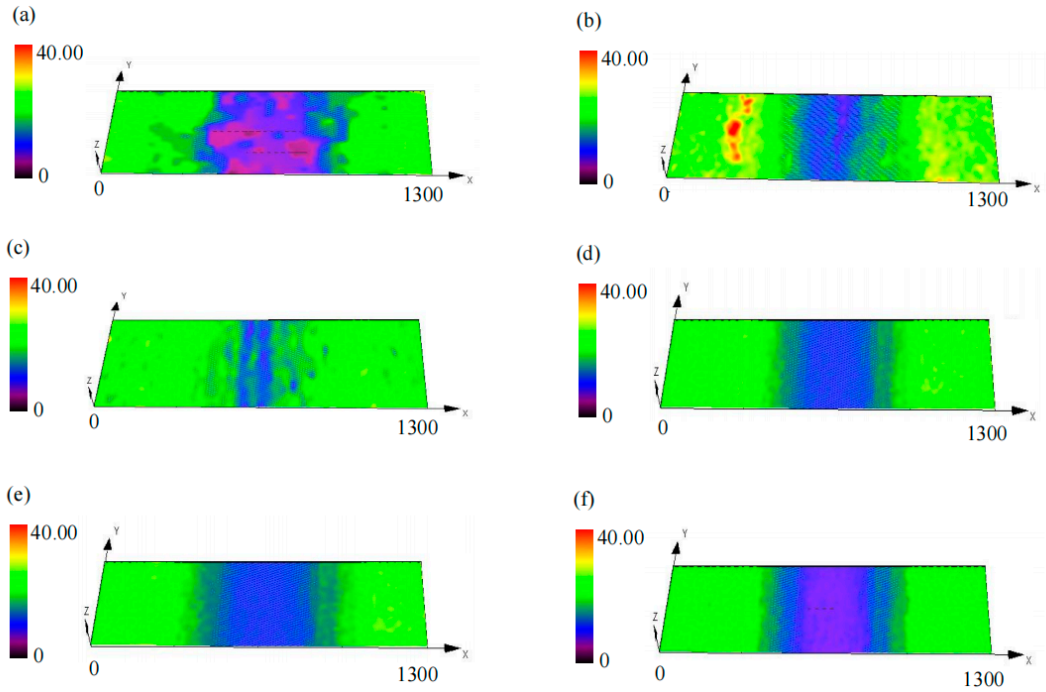

Figure 9. The 3D worn surface topographies after friction tests under 3 N load: (**a**) Seawater, (**b**) 0.1 mg/mL-PDA, (**c**) 0.25 mg/mL-PDA, (**d**) 0.5 mg/mL-PDA, (**e**) 0.75 mg/mL-PDA, (**f**) 1.0 mg/mL-PDA.

Overall, the experimental results demonstrated that the depth and width of the abrasion marks of UHMWPE disks, which reached their minimum values when the PDA content was 0.25 mg/mL, grew with increasing PDA content. When PDA content was increased to 1 mg/mL, micro-pit defects were evident on the wear surface of the UHMWPE disk, a phenomenon that coincides with the results and trends shown in Figure 9.

4. Discussion

The above experimental results demonstrate that the lubricating ability of seawater suspension with added PDA is significantly superior to that of seawater alone. In order to analyze the friction coefficient and surface wear characteristics more accurately, we further investigated the lubrication mechanism of PDA in a seawater environment. We conducted a detailed microstructural analysis of the wear surface.

Figure 9 illustrates the surface microstructure and elemental distribution of copper wear surfaces after friction under seawater conditions and seawater suspension with added PDA. As shown in Figure 10a, the friction surface of the copper material under seawater conditions exhibits pronounced plow grooves, along with numerous abrasive chips and spalling pits, indicating that abrasive wear is the predominant wear mechanism. There is no visible nitrogen on the surface, as seen in Figure 10b. The copper wear surface after friction in the seawater suspension with PDA added appears as a large black smoother area, as depicted in Figure 10c. Additionally, the furrows are relatively shallow and darker in color, appearing black. Figure 10d reveals that the black area is covered with nitrogen, a characteristic element of PDA, indicating that during friction, PDA ruptures and deforms

due to shear forces, eventually adhering to the copper surface and forming an adhesive layer with lubrication and wear-reducing properties. This film not only reduces direct contact and friction but also adsorbs and fills tiny pits in the surface, thus further reducing the coefficient of friction and wear. In other areas, nitrogen was detected, albeit at lower density, suggesting that the PDA component adhered to the surface to some extent. Even in areas of low N-element density, the presence of PDA components can still provide some protection, reducing friction and wear. These small amounts of attached PDA components may improve the overall tribological properties by forming a thin film on the surface that fills small pits and cracks.

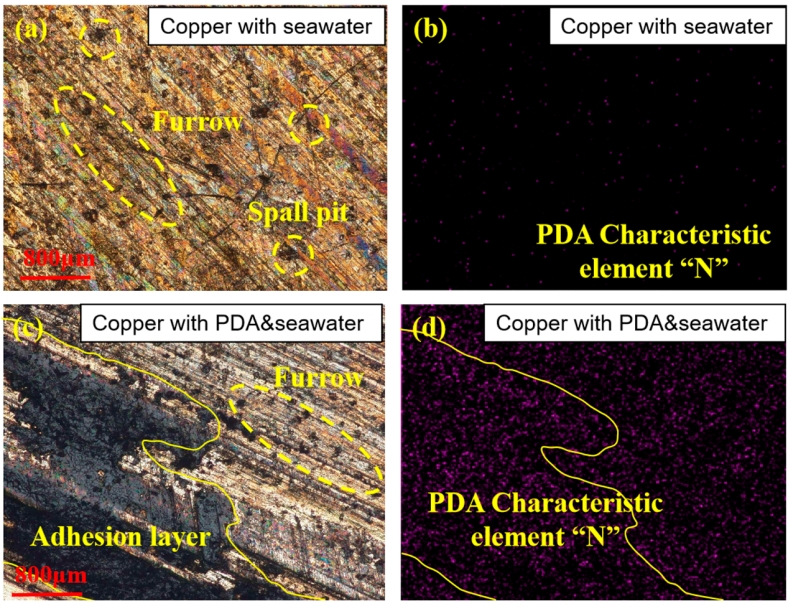

Figure 10. The SEM and nitrogen EDS images of copper friction pairs after rubbing tests (3 N). (**a**) Surface morphology of the Cu ball after friction in a seawater environment. (**b**) N element distribution on the surface of the Cu ball after friction in a seawater environment. (**c**) Surface morphology of the Cu ball after friction in a PDA & seawater suspension environment. (**d**) N element distribution on the surface of the Cu ball after friction in a PDA & seawater suspension environment.

Figure 11 demonstrates the surface micro-morphology of the UHMWPE disk lubricated with seawater PDA suspension. The UHMWPE disk lubricated with seawater PDA suspension exhibits a smoother friction surface with relatively shallower abrasion marks compared to the water-lubricated UHMWPE disk. This suggests that the seawater PDA suspension offers superior lubrication and protection for the UHMWPE disk. The absence of nitrogen on the friction surface of the UHMWPE disk indicates that the adhesion ability of PDA nanoparticles on the UHMWPE disk is very limited.

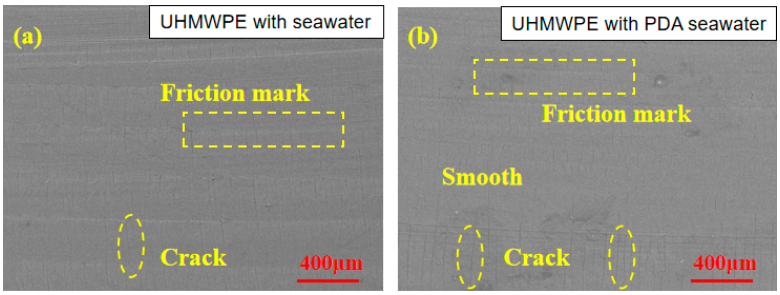

Figure 11. The SEM and nitrogen EDS images of UHMWPE friction pairs after rubbing tests (3 N). (**a**) Microscopic surface of UHMWPE after friction in a seawater environment. (**b**) Microscopic surface of UHMWPE after friction in a PDA & seawater environment.

Analyzing the comprehensive experimental results, we conclude that the tribological performance of the Cu–UHMWPE friction pair can be significantly enhanced by strategically incorporating PDA nanoparticles into dewatered seawater. To further elaborate on the effective reduction of frictional wear in PDA seawater suspensions, the lubrication mechanism of PDA materials is discussed.

It is universally acknowledged that direct contact with rough friction surfaces leads to localized plastic deformation and damage, which are key factors affecting the tribological properties of polymer materials [14]. According to Figure 10a,b, in a seawater environment, the water film has limited carrying capacity, and during the friction process, a large shear force will be generated, causing the liquid to be expelled from the contact area. This results in direct contact between the friction surfaces, leading to the formation of deeper ploughing grooves with abrasive particles. These rough grooves and crests with abrasive grains produce significant shear damage and deformation during friction, leading to higher frictional resistance and wear, as evidenced by higher friction coefficients and wear loss rates in the test results.

According to Figure 10a,b, the PDA seawater suspension demonstrates superior friction and wear performance compared to the seawater environment under identical test conditions. The furrows on the friction surfaces are shallower, with a relatively reduced number of abrasive grains and flaking pits. The most noteworthy observation is that under the frictional wear of the PDA seawater suspension, the surface of the copper ball develops a large, smooth region, and Figure 10d reveals that this smooth region contains a substantial amount of the characteristic PDA element: nitrogen. From this, it can be inferred that during the friction process, PDA generates an adhesion layer with lubricating and protective properties on the surface of the copper ball, and this adhesion layer plays a crucial role in the friction process.

Comprehensive experimental and test results reveal the lubrication mechanism of PDA seawater suspension, as illustrated in Figure 12. During the friction process, PDA nanoparticles are crushed or extruded into a thin film under the combined action of normal load and shear, adhering to the surface of the copper ball and forming a PDA adhesion layer.

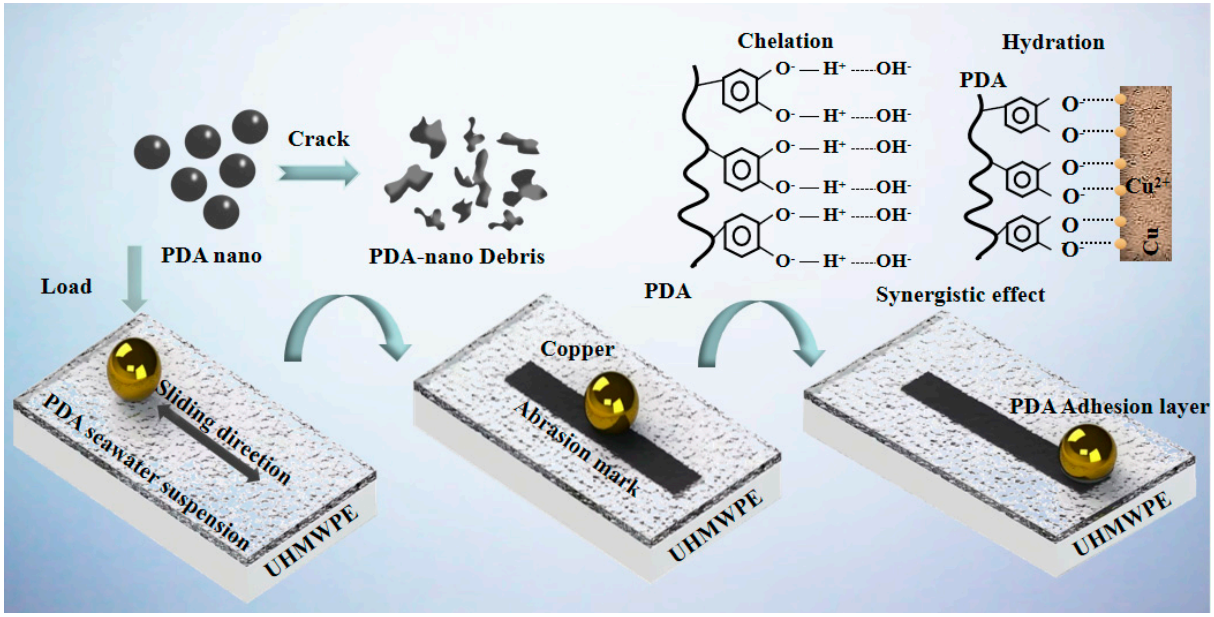

Figure 12. Analysis of the lubrication mechanism of PDA nanoparticles.

According to the current study, the catechol group on the PDA molecular chain exhibits excellent metal coordination with copper [23,24]. Consequently, PDA nanoparticles can quickly adhere to the surface of Cu balls, transferring directionally to the wear region during the friction process. Additionally, free PDA nanoparticles in seawater can

continuously adhere to bare friction surfaces damaged by shear forces during friction [25]. This property endows the PDA lubrication film with excellent directional transfer and self-healing capabilities. Likewise, it has been proved that the hydroxyl groups on the PDA molecular chain are charged in liquid environments and can form hydrogen bonds with polar water molecules [26], as shown in Figure 11. These water molecules are attracted to the surface of the PDA membrane and gradually penetrate into the membrane through its microporous structure [25]. Consequently, the microporous structure of the PDA film becomes saturated with free water molecules, providing excellent hydration lubrication during friction.

Based on the above analysis, the PDA adhesion layer on the surface of the copper balls exerts two pivotal influences on enhancing the tribological performance of the mating pair. First, the PDA nanoparticles, crushed and extruded during the friction process, fill the exfoliation pits and abrasion marks on the copper ball's surface, thereby reducing the depth of abrasion marks, forming an adhesion layer, and minimizing plastic deformation and fracture behaviors induced by the interaction of micropeaks with shear forces on the two friction surfaces, all of which simultaneously enhance stability. This process reduces frictional resistance and wear rate, thereby improving the tribological performance of the friction pair. On the other hand, the hydrogen bonding of PDA nanoparticles with an alkaline environment due to electronegativity difference can improve the stability and lubricity of the lubrication film to a certain extent, as shown in Figure 12 [24,25]. Therefore, the PDA film adhered to the surface of the copper balls can significantly reduce the friction factor-to-wear ratio in the experimental tests.

5. Conclusions

In this paper, PDA nanoparticles that improve the lubrication performance of aqueous film were prepared, and the tribological behavior between copper spheres and UHMWPE disks in a seawater environment was systematically tested and analyzed. Additionally, through comprehensive analysis of the experimental results, the lubrication mechanism of PDA nanoparticles in a seawater environment was proposed. The main conclusions of this paper are as follows:

(1) PDA nanoparticles effectively enhance the lubricating ability of seawater under almost all experimental conditions, with the optimal concentration of PDA nanoparticles being 0.25 mg/mL;
(2) Compared to the seawater environment, PDA nanoparticle seawater suspensions exhibit superior lubricating abilities, characterized by a lower friction coefficient, reduced wear rate, and smoother surface wear;
(3) Compared to UHMWPE disks, PDA nanoparticles exhibit stronger adhesion on the worn surface of copper balls. A large adhesive layer is observed, and the adhesion strength between PDA and copper balls is sufficient to withstand frictional shear forces. Conversely, the adhesion strength between PDA and UHMWPE disks is relatively weaker, making it challenging to withstand strong shear forces during friction;
(4) The synergistic effect of the biomimetic adhesion and hydration lubrication of PDA nanoparticles is the primary mechanism for enhancing tribological performance, ensuring long-lasting, stable, and targeted water lubrication throughout the friction process.

Author Contributions: Data curation, Y.X.; Writing—original draft, X.Z.; Writing—review & editing, C.W.; Project administration, Z.G. All authors have read and agreed to the published version of the manuscript.

Funding: This work was supported by the Shaanxi Provincial Natural Science Foundation (No. 2023-JC-YB-346), Shaanxi Provincial Qinchuangyuan High-level Talent Program (No. QCYRCXM-2023-105), Scientific Research Program Funded by Shaanxi Provincial Education Department (Program No. 22JC009), and Fund of National Engineering Research Center for Water Transport Safety (No. A202304).

Data Availability Statement: Data are contained within the article.

Conflicts of Interest: The authors declare no conflict of interest.

References

1. Liu, Q.; Ouyang, W.; Cheng, Q.; Li, J.; Cheng, Q.; Li, R. Influences of bidirectional shaft inclination on lubrication and dynamic characteristics of the water-lubricated stern bearing. *Mech. Syst. Signal Process.* **2022**, *169*, 108623. [CrossRef]
2. Lin, C.G.; Zou, M.S.; Zhang, H.C.; Qi, L.B.; Liu, S.X. Influence of different parameters on nonlinear friction-induced vibration characteristics of water lubricated stern bearings. *Int. J. Nav. Archit. Ocean. Eng.* **2021**, *13*, 746–757. [CrossRef]
3. Jin, L.; Scheerer, H.; Andersohn, G.; Oechsner, M.; Hellmann, D. Experimental study on the tribochemical smoothening process between self-mated silicon carbide in a water-lubricated surface-contact reciprocating test. *Friction* **2018**, *7*, 181–191. [CrossRef]
4. Savio, D.; Falk, K.; Moseler, M. Slipping domains in water-lubricated microsystems for improved load support. *Tribol. Int.* **2018**, *120*, 269–279. [CrossRef]
5. Yang, Z.; Guo, Z.; Yang, Z.; Wang, C.; Yuan, C. Study on tribological properties of a novelcomposite by filling microcapsules into UHMWPE matrix for water lubrication. *Tribol. Int.* **2021**, *153*, 106629. [CrossRef]
6. McGhee, E.O.; Pitenis, A.A.; Urueña, J.M.; Schulze, K.D.; McGhee, A.J.; O'Bryan, C.S.; Bhattacharjee, T.; Angelini, T.E.; Sawyer, W.G. In situ, measurements of contact dynamics in speed-dependent hydrogel friction. *Biotribology* **2018**, *13*, 23–29. [CrossRef]
7. Cao, Y.; Kampf, N.; Kosinska, M.K.; Steinmeyer, J.; Klein, J. Interactions between bilayers of phospholipids mixture extracted from human osteoarthritic synovial fluid. *Biotribology* **2021**, *25*, 100157. [CrossRef]
8. Wang, C.; Bai, X.; Guo, Z.; Dong, C.; Yuan, C. A strategy that combines a hydrogel and graphene oxide to improve the water-lubricated performance of ultrahigh molecular weight polyethylene. *Compos. Part A Appl. Sci. Manuf.* **2021**, *141*, 106207. [CrossRef]
9. Mu, L.W.; Feng, X.; Shi, Y.J.; Wang, H.Y.; Lu, X.H. Friction and Wear Behaviors of Solid Lubricants/Polyimide Composites in Liquid Mediums. *Mater. Sci. Forum* **2010**, *654–656*, 2763–2766. [CrossRef]
10. Seror, J.; Zhu, L.; Goldberg, R.; Day, A.J.; Klein, J. Supramolecular synergy in the boundary lubrication of synovial joints. *Nat. Commun.* **2015**, *6*, 6497. [CrossRef]
11. Lee, S.L. A Proposed Model of Boundary Lubrication by Synovial Fluid: Structuring of Boundary Water. *J. Biomech. Eng.* **2010**, *101*, 185. [CrossRef]
12. Xue, G.; Zhang, Y.; Xie, T.; Zhang, Z.; Liu, Q.; Li, X.; Gou, X. Cell adhesion-mediated piezoelectric self-stimulation on polydopamine-modified poly(vinylidene fluoride) membranes. *ACS Appl. Mater. Interfaces* **2021**, *13*, 17361–17371. [CrossRef] [PubMed]
13. Kim, S.J.; Lee, S.; Kim, C.; Shin, H. One-step harvest and delivery of micropatterned cell sheets mimicking the multi-cellular microenvironment of vascularized tissue. *ActaBiomater* **2021**, *132*, 176–187. [CrossRef] [PubMed]
14. Sa, R.; Wei, Z.; Yan, Y.; Wang, L.; Wang, W.; Zhang, L.; Ning, N.; Tian, M. Catechol and poxy functionalized ultrahigh molecular weight polyethylene (UHMWPE) fibers with improved surface activity and interfacial adhesion. *Compos. Sci. Technol.* **2015**, *113*, 54–62. [CrossRef]
15. Huang, M.; Yao, Z.; Wu, Q.; Zheng, Y.; Liu, J.; Li, C. Robustness-heterogeneity-induced ultrathin 2D structure in Li plating for highly reversible Li-metal batteries. *ACS Appl. Mater. Interfaces* **2020**, *12*, 46132–46145. [CrossRef]
16. Zhang, W.; Yang, F.K.; Han, Y.; Gaikwad, R.; Leonenko, Z.; Zhao, B. Surface and tribological behaviors of the bioinspired polydopamine thin films under dry and wet conditions. *Biomacromolecules* **2013**, *14*, 394–405. [CrossRef]
17. Songfeng, E.; Shi, L.; Guo, Z. Tribological properties of self-assembled gold nanoparticles on silicon with polydopamine as the adhesion layer. *Appl. Surf. Sci.* **2014**, *292*, 750–755.
18. Ou, J.; Wang, Y.; Li, C.; Wang, F.; Xue, M.; Wang, J. Tribological behaviors of a novel trilayer nanofilm: The influence of outer chain length and interlayer thickness. *Surf. Interface Anal.* **2013**, *45*, 1182–1187. [CrossRef]
19. Mi, Y.; Wang, Z.; Liu, X.; Yang, S.; Wang, H.; Ou, J.; Li, Z.; Wang, J. A simple and feasible in-situ reduction route for preparation of graphene lubricant films applied to a variety of substrates. *J. Mater. Chem.* **2012**, *22*, 8036. [CrossRef]
20. Ou, J.; Liu, L.; Wang, J.; Wang, F.; Xue, M.; Li, W. Fabrication and Tribological Investigation of a Novel Hydrophobic Polydopamine/Graphene Oxide Multilayer Film. *Tribol. Lett.* **2012**, *48*, 407–415. [CrossRef]
21. Chen, J.; Zhang, J.; Hu, M.; Zheng, Z.; Wang, K.; Li, X. Preparation of Ni/graphene hydrophobic composite coating with micro-nano binary structure by poly-dopamine modification. *Surf. Coat. Technol.* **2018**, *353*, 1–7. [CrossRef]
22. Wang, C.; Bai, X.; Dong, C.; Guo, Z.; Yuan, C. Friction properties of polyacrylamide hydrogel particle/HDPE composite under water lubrication. *Polymer* **2019**, *180*, 121703. [CrossRef]
23. Chen, G.; Jin, B.; Zhao, J.; Li, Y.; He, Y.; Luo, J. Efficient one-pot synthesis of mussel-inspired Cu- doped polydopamine nanoparticles with enhanced lubrication under heavy loads. *Chem. Eng. J.* **2021**, *426*, 131287. [CrossRef]
24. Wu, L.; Zhang, Z.; Yang, M.; Yuan, J.; Li, P.; Chen, Z.; Men, X. Surface modification of YS-20 with polydopamine for improving the tribological properties of polyimide composites. *Friction* **2022**, *10*, 411–421. [CrossRef]

25. Chen, G.; Zhao, J.; Chen, K.; Liu, S.; Zhang, M.; He, Y.; Luo, J. Ultrastable lubricating properties of robust self-repairing tribofilms enabled by in situ-assembled polydopamine nanoparticles. *Langmuir* **2020**, *36*, 852–861. [CrossRef]
26. Tian, Q.; Jia, X.; Yang, J.; Wang, S.; Li, Y.; Shao, D.; Song, H. Polydopamine-stabilized ZIF-8: Improved water stability and lubrication performance. *Appl. Surf. Sci.* **2022**, *578*, 152120. [CrossRef]